Geoscience Frontiers xxx (xxxx) xxx

HOSTED BY

Contents lists available at ScienceDirect

Geoscience Frontiers

journal homepage: www.elsevier.com/locate/gsf

Dehydration melting of amphibolite at 1.5 GPa and 800–950 °C: Implications for the Mesozoic potassium-rich adakite in the eastern North China Craton

Zhilin Ye [a,b], Fang Wan [c], Neng Jiang [d], Jingui Xu [a], Yuanyun Wen [e], Dawei Fan [a,*], Wenge Zhou [a]

[a] Key Laboratory of High-Temperature and High-Pressure Study of the Earth's Interior, Institute of Geochemistry, Chinese Academy of Sciences, Guiyang, 550081, China
[b] University of Chinese Academy of Sciences, Beijing, 100049, China
[c] Minco International Mining Consulting Ltd., Beijing, 100012, China
[d] Institute of Geology and Geophysics, Chinese Academy of Sciences, Beijing, 100029, China
[e] Center for Lunar and Planetary Sciences, Institute of Geochemistry, Chinese Academy of Sciences, Guiyang, 550081, China

ARTICLE INFO

Keywords:
Amphibolite
Partial melting
Eastern North China Craton
Potassium-rich adakitic rocks
Hannuoba granulite xenoliths

ABSTRACT

Mesozoic intermediate-felsic magmatic rocks in the eastern North China Craton commonly show geochemical similarity to adakites. However, the lack of direct constraints from partial melting experiments at high pressures and temperatures fuels a debate over the origin of these rocks. In this work, we performed partial melting experiments at 1.5 GPa and 800–950 °C on amphibolite samples collected from the vicinity of the Mesozoic potassium-rich adakitic rocks in the Zhangjiakou area, northern margin of the North China Craton. The experimental melts range from granitic to granodioritic compositions, with SiO_2 = 56.4–72.6 wt.%, Al_2O_3 = 16.1–19.3 wt.%, FeO* = 2.4–9.6 wt.%, MgO = 0.3–2.0 wt.%, CaO = 0.6–3.8 wt.%, Na_2O = 4.7–5.3 wt.%, and K_2O = 2.6–3.9 wt.%, which are in the ranges of the surrounding Mesozoic potassium-rich adakitic rocks, except for the higher Al_2O_3 contents and the data point at 1.5 GPa and 800 °C. Trace element compositions of the melts measured by LA-ICP-MS are rich in Sr (849–1067 ppm) and light rare earth elements (LREEs) and poor in Y (<10.4 ppm) and Yb (<0.88 ppm), and have high Sr/Y (102–221) and $(La/Yb)_n$ (27–41) ratios and strongly fractionated rare earth element (REE) patterns, whereas no obvious negative Eu anomalies are observed. The geochemical characteristics show overall similarity to the Mesozoic potassium-rich adakitic rocks in the area, especially adakites with low Mg#, again except for the data point at 1.5 GPa and 800 °C. The results suggest that partial melting of amphibolite can produce potassium-rich adakitic rocks with low Mg# in the eastern North China Craton under the experimental conditions of 1.5 GPa and 850–950 °C. The experimental restites consist of hornblende (Hbl) + plagioclase (Pl) + garnet (Grt) ± clinopyroxene (Cpx), a mineral assemblage significantly different from that of the nearby Hannuoba mafic granulite xenoliths which consist of Cpx + orthopyroxene (Opx) + Pl ± Grt. Chemically, the experimental restites contain higher Al_2O_3 but lower MgO and CaO than the Hannuoba mafic granulite xenoliths. We therefore argue that the Hannuoba mafic granulite xenoliths cannot represent the direct products of partial melting of the experimental amphibolite.

1. Introduction

Adakites were initially defined as products of melting subducted young, hot oceanic crust (Kay, 1978; Defant and Drummond, 1990) and are characterized by elevated contents of Na_2O, Al_2O_3, strontium and light rare earth elements (LREEs) and depleted heavy rare earth elements (HREEs) and yttrium (Y). Meanwhile, some studies have indicated that adakites may also be derived from slab melts modified by interactions with the overlying mantle wedge peridotite (e.g., Kay, 1978; Sato et al., 2013). Moreover, as more data accumulated, they show that adakitic rocks can also form where the subducted oceanic crust is old and thus inferred to be cold (Macpherson et al., 2006).

In addition, some adakitic rocks are not related to oceanic crust subduction. Instead, they may represent partial melting of newly

* Corresponding author.
E-mail addresses: fandawei@vip.gyig.ac.cn (D. Fan), zhouwenge@vip.gyig.ac.cn (W. Zhou).
Peer-review under responsibility of China University of Geosciences (Beijing).

https://doi.org/10.1016/j.gsf.2020.03.008
Received 10 September 2019; Received in revised form 20 February 2020; Accepted 20 March 2020
Available online xxxx

underplated crust or thickened mafic lower continental crust (e.g., Atherton and Petford, 1993; Wang et al., 2005) or interaction between partial melts of foundered lower continental crust and mantle peridotite (e.g., Xu et al., 2002, 2008; Gao et al., 2004; Liu et al., 2005).

In the eastern North China Craton, there are widespread geochemical similarities between Mesozoic intermediate-felsic magmatic rocks and adakites (e.g., Jiang et al., 2007; Chen et al., 2013; He et al., 2017; Ding et al., 2019). However, many of these rocks are distinctly potassium-rich and have been termed potassium-rich adakites (Rapp et al., 2002). In addition, they have evolved strontium, neodymium, and hafnium isotope compositions as well as abundant Precambrian inherited zircons and lack evidence of interaction with mantle peridotite (e.g., Jiang et al., 2007; Yang et al., 2016; Liu et al., 2018; Ding et al., 2019). Some previous studies argued that adakitic rocks with high Mg# signatures are products of the interaction of partial melt of (foundered) lower continental crust with mantle peridotite (Gao et al., 2004; Liu et al., 2005; Xu et al., 2008). However, other studies have suggested that adakitic rocks with relatively low Mg# signatures may be derived from partial melting of the lower crust (e.g., Jiang et al., 2007; Huang and He, 2010; Xiong et al., 2011; Ma et al., 2015; Yang et al., 2016; Liu et al., 2018; Ding et al., 2019). Furthermore, some previous studies indicated that adakitic rock and granulite xenoliths in Neogene basalt may share a common petrogenesis (Liu et al., 2005; Jiang et al., 2007). For example, Jiang et al. (2007) proposed that potassium-rich adakitic rocks in the Zhangjiakou area on the northern margin of the North China Craton formed by partial melting of ancient lower crust that could be represented by exposed Precambrian granulites and amphibolites and that some of the Hannuoba mafic granulite xenoliths could be restites of partial melting events. In contrast, Liu et al. (2005) believed that intermediate-mafic granulite xenoliths with high Mg# and Ni content formed by silicic melts of lower crustal rock reacting with mantle peridotite. Due to the complexity of potassium-rich adakitic rocks and granulite xenoliths, however, field observations alone cannot completely resolve their genesis.

On the other hand, few experiments have been carried out to constrain the origin of adakites (e.g., Sen and Dunn, 1994; Rapp and Watson, 1995; Qian and Hermann, 2013). Although experimental studies have shown that 10%–30% melting of variably hydrated basaltic rocks at pressures of 1–4 GPa and temperatures of 850–1000 °C can produce liquids similar to adakites in terms of their major element components, trace element data for experimental liquids are relatively scarce. Furthermore, the initial materials used in all experiments to date have no relation with adakites in time and space. Therefore, the proposal that potassium-rich adakitic rocks in the North China Craton formed by partial melting of the ancient lower crust has not been confirmed by partial melting experiments at high pressure and high temperature.

In this paper, we experimentally investigate whether partial melting of the exposed Precambrian amphibolites at high pressure and high temperature can produce rocks with potassium-rich adakitic signatures and whether the experimental restites are similar to the presumed restitic Hannuoba mafic granulite xenoliths. The partial melting experiments were carried out at a pressure of 1.5 GPa and temperatures from 800 °C to 950 °C. Both the major and trace elements in the resulting partial melts were compared with those of the exposed potassium-rich adakitic rocks, and the experimental restites were further compared with the Hannuoba mafic granulite xenoliths to provide constraints on the origins of potassium-rich adakitic rocks and Hannuoba mafic granulite xenoliths.

2. Starting material and experimental and analytical procedures

The starting material (JN0305e) is an amphibolite from the vicinity of the Guzuizi granite in the Zhangjiakou area, northern margin of the North China Craton (Fig. 1). The amphibolite is massive and dark-gray and has strong foliations and chloritic alteration. The rock is roughly composed of 45% plagioclase (Pl), 25% chlorite (Chl), 15% hornblende (Hbl), 5% augite, and trace amounts of magnetite (3%), titanite (5%) and others (2%). The grain size of the minerals is less than 0.5 mm. The chemical compositions of rock and major minerals are reported in Table 1.

The amphibolite was ground parallel to the foliation into a cylindrical core that was 4.0 mm in diameter and 2.5 mm in length. The samples were then washed in alcohol with an ultrasonic-washer and placed in an oven at 150 °C for at least 12 h in order to eliminate moisture from the sample.

Experiments were conducted at 1.5 GPa and 800–950 °C in a multi-anvil pressure apparatus, YJ-3000t press, at the Institute of Geochemistry, Chinese Academy of Sciences. A detailed description of the system was presented by Xie et al. (1993). The massive sample was placed in a graphite capsule. The graphite capsule was enclosed in a gold capsule, which was later soldered. Then, the graphite-lined gold capsule was placed in a pyrophyllite capsule blocked by pyrophyllite columns at the two ends. The pyrophyllite cube and stainless steel foil were used as a pressure-transmitting medium and a heater, respectively. The pyrophyllite capsules, columns, and cubes were heated to 800 °C to remove the absorbent water before the experiments.

The experimental temperature measurement, pressure calibration, and oxygen fugacity were identical to those that used by Zhou et al. (2005). The experimental path consisted of initial compression at room temperature followed by a series of heating cycles at constant pressure. First, we increased the pressure at a rate of 4×10^5 Pa/s. After holding the pressure at 1.5 GPa for approximately 10 min, we increased the temperature at a rate of 10 °C/s to the goal temperature and then held it constant for approximately 100 h. The temperature was continuously recorded during the experiments. The fluctuation in temperature read from the thermocouple was within ±5 °C during the whole process. When runs were over, the samples were quenched by turning off the power to the apparatus. Then, the recovered products of the experiment were sectioned and polished for observation and analysis under a microscope and microprobe.

The experimental conditions and mineral components of the run products are listed in Table 1. The major element compositions of run products (Table 1) were measured by EPMA-1600 electron microprobe (EMP) analysis at the Institute of Geochemistry, Chinese Academy of Sciences. The operating conditions were an acceleration voltage of 15 kV, a beam current of 20 nA, a peak counting time of 10 s, and beam diameters of 5 μm and 10 μm for mineral and melt analyses, respectively. Na and K were the first and second elements to be analyzed in order to avoid the Na- and K-loss problems in the EMP analyses (Morgan and London, 2005). Trace element compositions of some melts (Table 2) were measured at China University of Geosciences, Wuhan by LA-ICP-MS (GeolasPro + Agilent 7500a, $\lambda = 193$ nm), with spot sizes of 24–44 μm, an energy density 15 cm^2/mJ, an HV of 80 kV, an energy of 23.8 mJ, and a repeat frequency of 8 Hz. We used Si as the internal standard for melts in data processing by the Glitter software (Gao et al., 2002). The accuracy of analyses of trace elements was within ±10%.

3. Results

3.1. Characteristics of run products

3.1.1. Melt distribution

Although melts appear in all run products, significant melting does not begin until approximately 900 °C and only a few melt pools appear in the runs at 800–850 °C. Thin films of melts emerge between Hbl and Pl in fissures and along cleavage planes of these minerals. The amounts of melts are too small to form interconnections, so the whole structure of the rock is not significantly changed (Fig. 2a and b). At 900 °C, a belt of melt appears around mineral grains and begins to interconnect (15 wt.%), showing a clear embed-erode texture (Fig. 2c). In the 950 °C run, the melt is extensive and occupies many areas in the image (Fig. 2d), with the residual minerals distributed as conglomerations in the melt.

3.1.2. Assemblage of restites

At 800 °C, all Chl becomes Hbl. In addition to initial Pl and Hbl, some foliar clinopyroxene (Cpx) and orthopyroxene (Opx) are present in the restite (Fig. 2a). The restites of the 850 °C and 900 °C runs are similar to each other, containing Pl, Hbl, and fresh garnet (Grt), which is usually found among Pl and Hbl (Fig. 2b and c). Restite at 950 °C contains Hbl, Grt, and Cpx. The disappearance of Pl suggests that it has been completely consumed. The garnet is larger than those from the 850 °C and 900 °C runs, is present between melt and Hbl and interconnects to Hbl (Fig. 2d), which reflects the reactive relationship between them. Cpx is disseminated in Hbl and very difficult to identify in backscattered electron images.

3.2. Melt compositions

The hydrous minerals that begin to dehydrate at 800 °C in our starting material (such as Hbl and Chl) are relatively abundant. However, the dehydration temperature is lower than those of previous studies (Rapp et al., 1991; Wolf and Wyllie, 1991; Sen and Dunn, 1994; Winther, 1996; Zhou et al., 2005) under similar pressure because of the low dehydration temperature of Chl. All the gross wt.% values of the melts derived from electron microprobe analysis are in the range of 92%–94%, perhaps due to the melts containing much water. Thus, we first normalize the data them to 100% (anhydrous basis), using the method described previously (Sen and Dunn, 1994) and then proceed with further discussion.

Fig. 3 shows the major element compositions of melts versus temperature. With increasing temperature, the SiO_2 contents decrease from 72.6% (800 °C) to 56.4% (950 °C), showing that the overall composition of the melts changes from silicic to intermediate. The contents of Al_2O_3 are low at 800 °C (16.1%), increase gradually at 850–900 °C (18.1%–18.6%) and reach a maximum at 950 °C (19.1%). The FeO* contents remain constant from 800 to 850 °C at first, then increase gradually from 2.0% to 3.1% in the range of 850–900 °C, and finally increase rapidly to 9.6% at 950 °C. The variation trend of MgO content is the same as that of FeO* content, remaining constant at 0.3% from 800 to 850 °C, then increasing to 0.4% at 900 °C, and finally increasing rapidly to 2.1% at 950 °C. Similar to FeO* and MgO, the contents of CaO and TiO_2 are stable at first, then increase slowly and at the end increase rapidly. Their ranges are 0.6%–3.8% and 0.1%–0.9%, respectively. The variation behavior of the Na_2O content is similar to that of SiO_2 content, decreasing from 5.3% (800 °C) to 4.7% (950 °C). However, the variation range of K_2O content, which increases at 800–850 °C from 2.6% to 3.9% and then decreases slowly to 2.9% at 950 °C, is slightly different from those of the other oxides. In summary, except for the contents of Al_2O_3, K_2O and Na_2O, the contents of the other oxides vary slightly at temperatures below 900 °C but significantly when the temperature exceeds 900 °C, which may be the result of accelerated melting of Hbl at higher temperatures.

In the albite (Ab)–anorthite (An)–orthoclase (Or) diagram (Fig. 4), the run melt compositions evolve from trondhjemite to granite and finally to granodiorite with increasing temperature. The melt component trend in Fig. 4 indicates that the normative An contents increase at temperatures ranging from 800 °C to 950 °C (4.6%–23.6%) and that the normative Ab contents decrease gradually (71.2%–53.5%), while the normative Or contents increase from 800 to 850 °C (24.2%–32.6%) and then decrease from 850 to 950 °C (32.6%–22.9%). These trends are similar to those of the run melts by Sen and Dunn (1994) but different

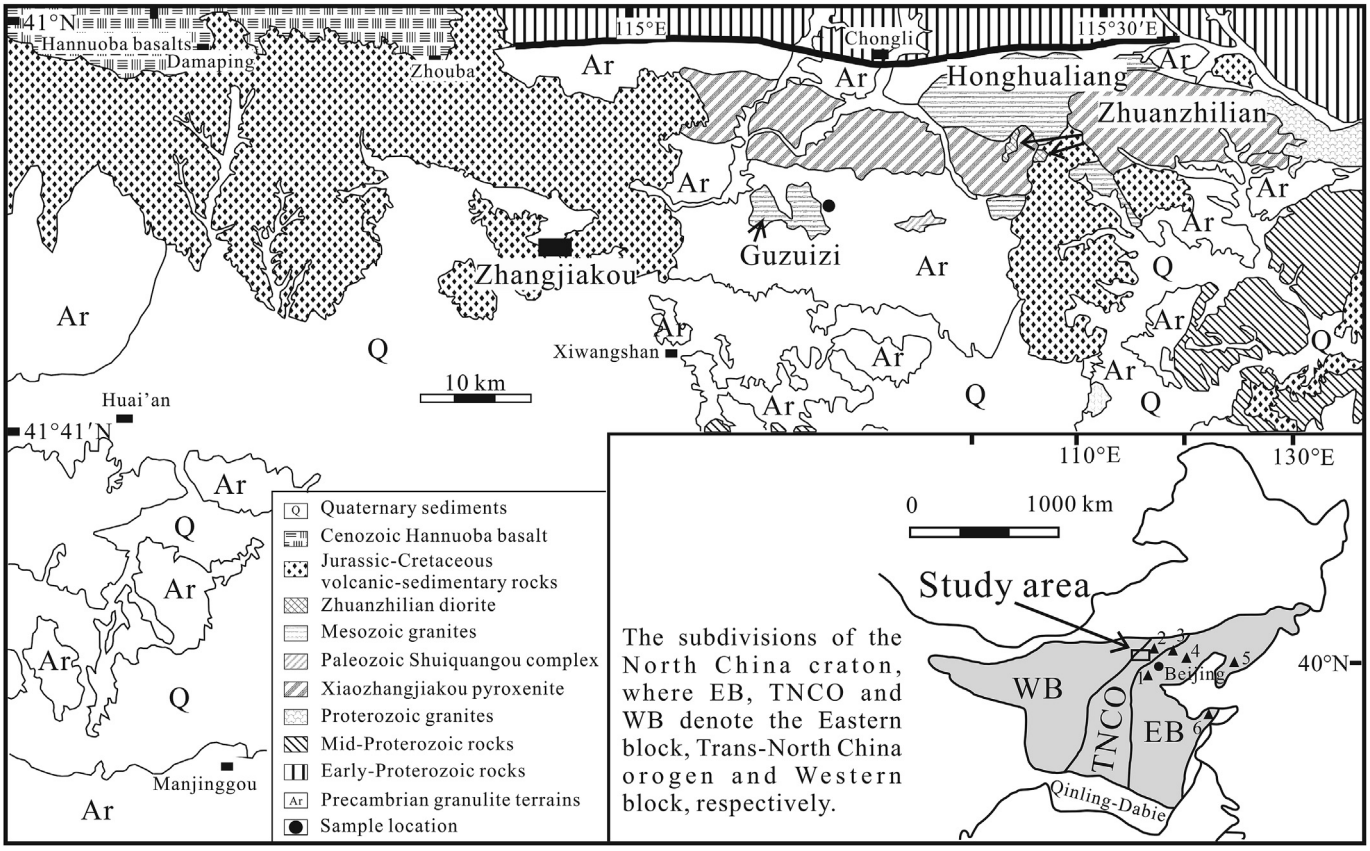

Fig. 1. Simplified geological map of the Zhangjiakou area showing the distributions of the Mesozoic potassium-rich adakitic rocks, the granulite xenolith-bearing Hannuoba basalts and the granulite terrains. The solid triangles in the inset show the locations of Mesozoic potassium-rich adakitic rocks from other parts of the eastern North China Craton: 1, Fangshan granodiorite in southwestern Beijing; 2, volcanic rocks of the Tiaojishan Formation in western Beijing; 3, volcanic rocks of the Tiaojishan Formation in northern Hebei Province; 4, Dushan granite in northern Hebei Province; 5, granitoids (including the Xiaoheishan quartz diorite and granodiorite, the southern Hanjialing granodiorite, the Yutun quartz diorite and the Jiuliancheng monzogranite) in eastern Liaoning Province; and 6, Guojialing granodiorite in eastern Shandong Province. Modified from Jiang et al. (2007).

from those of run melts by Rushmer (1991), Wolf and Wyllie (1994) and Rapp and Watson (1995), which are trondhjemitic and tonalitic in composition. Differences in the composition and water content of the starting material may be the primary reasons for this diversity.

3.3. Restite compositions

The Pl in the starting material is Ab (An content 9.1%). At 800 °C, the contents of An in Pl and melt are 9.4% and 4.8%, respectively. With temperature increasing from 800 °C to 900 °C, the contents of An in Pl and melt increase gradually from 9.4% to 17.2% and 4.8%–13.3%, respectively. At 950 °C, Pl is completely consumed, and the content of An in the melt is 23.6%.

All run products contain Hbl (Table 1). Hbl compositions are more variable in the lower temperature runs (T < 950 °C) than in the 950 °C run. The Si and Mg atoms per formula unit fluctuate (the formula is calculated by the method of Hawthorne et al. (2012)). With increasing temperature, the Si atoms decrease from 6.45 to 6.11, and Mg atoms increase from 1.88 to 2.65.

Grt appears in the 850–950 °C runs. The Grt grains are relatively homogeneous in composition within a given experimental charge (Table 1). The change in composition with temperature is obvious (Table 1). As a whole, with increasing temperature, the almandine contents decrease (60.4–47.9–48.2 mol.%), pyrope contents increase (23.4–44.8–31.8 mol.%) and grossular contents fluctuate significantly (13.7–6.3–17.8 mol.%).

Cpx is found in the 800 °C and 950 °C runs and consists of 19.2 mol.% jadeite (Jd) + 28.5 mol.% $CaSiO_3$ (Wo) + 16.9 mol.% enstatite (En) + 35.4 mol.% ferrosilite (Fs) and 13.7 mol.% Jd + 35.4 mol.% Wo + 28.6 mol.% En + 22.3 mol.% Fs, respectively. Opx appears at 800 °C and is low in content. The main constituent of Opx is 40 mol.% En + 60 mol.% Fs.

4. Discussion

4.1. Equilibrium

The reversed vapor-absent partial melting experiments on powdered amphibolites carried out by Beard and Lofgren (1991) demonstrated that isothermal runs of 96 h duration were sufficient to produce reasonable equilibrium melts and mineral assemblages at temperatures as low as 900 °C. However, time-dependent runs with powdered amphibolites conducted by Zhang et al. (2013) indicated that near-equilibrium mineral assemblages were obtained in experiments if experimental durations were ≥8 days at temperatures ≥800 °C. Moreover, dehydration-melting experiments with solid amphibolite conducted by Wolf and Wyllie (1991) demonstrated that even when the experimental duration is as long as 21 days, the mineral assemblage may not achieve equilibrium. Although solid amphibolite was used as the starting material in our experiments, this starting material contained Chl, which means that it contained more water and could be dehydrated at relatively low temperatures. Moreover, the durations of our runs were longer than 96 h (Table 1). As shown in Table 1, Grt and Hbl produced in runs below 950 °C were obviously heterogeneous in composition. Meanwhile, the melts were physically localized, heterogeneous in composition and not completely interconnected. Thus, these runs did not achieve a close approach to equilibrium. However, the minerals in our 950 °C runs were reasonably homogeneous. We conclude that our 950 °C experiment was acceptably close to equilibrium.

4.2. Reactions

The reactions in the dehydration melting process of amphibolite are complex and affected by many factors, such as mineral composition, pressure, temperature, and fluid content. Generally, the overall reaction

Table 1
Main constituents and major element compositions of starting material and experimental products.[a]

	SiO_2	TiO_2	Al_2O_3	FeO*	MnO	MgO	CaO	Na_2O	K_2O	P_2O_5	Total
JN0305e (starting material)											
Bulk rock	44.5	1.94	14.17	12.33	0.21	5.81	7.26	4.73	1.3	0.08 Cr_2O_3:0.71	99.36 (LOI: 6.31)
Hbl(6)	40.98(83)	0.93(16)	10.20(64)	20.18(59)	0.38(3)	8.16(44)	9.13(38)	2.79(11)	1.77(19)	0.01(1)	94.53(104)
Pl(7)	65.65(96)	0.01(2)	20.61(56)	0.08(2)	0.01(1)	0.00(0)	1.89(56)	10.38(52)	0.15(4)	0.01(1)	98.78(41)
Chl(3)	30.47(60)	1.06(21)	14.68(19)	23.99(49)	0.41(6)	13.39(37)	0.14(4)	0.04(2)	3.68(6)	0.00(0)	87.87(61)
JN0305e-4k 800°C 1.5 GPa 100 h 0.45Hbl + 0.4Pl + 0.08Cpx + 0.05Opx + 0.02Gl											
Hbl(3)	44.01(121)	0.66(5)	12.84(158)	17.43(106)	0.33(6)	9.49(59)	6.29(63)	4.07(21)	0.57(1)	0.06(6)	95.74(38)
Pl(7)	66.04(56)	0.01(1)	20.98(34)	0.29(13)	0(0)	0(0)	1.98(28)	10.35(25)	0.28(11)	0.05(8)	99.99(85)
Cpx(2)	52.55(33)	0.16(2)	1.05(19)	23.22(489)	0.7(11)	6.43(22)	13.11(209)	2.81(86)	0(0)	0.02(3)	100.03(165)
Opx(6)	51.86(71)	0.09(5)	0.72(17)	34.29(132)	0.39(7)	12.3(78)	1.29(68)	0.33(17)	0.01(1)	0.03(2)	101.33(105)
Gl(6)	68.13(104)	0.04(3)	15.10(80)	2.22(80)	0.03(2)	0.25(14)	0.55(19)	4.99(56)	2.43(19)	0.08(11)	93.83(104)
JN0305e-1k 850°C 1.5 GPa 97 h 0.5Hbl + 0.4Pl + 0.02Grt + 0.08Gl											
Hbl(6)	41.92(71)	1.5(87)	14.67(226)	16.52(251)	0.21(1)	8.43(42)	8.52(57)	3.42(52)	1.27(29)	0.02(1)	96.47(100)
Pl(10)	65.12(121)	0.03(2)	21.79(79)	0.17(15)	0.01(1)	0.01(2)	3.14(84)	9.47(81)	0.77(44)	0.03(2)	100.54(62)
Grt(6)	40.07(100)	0.11(4)	20.39(32)	28.23(129)	1.14(11)	6.15(55)	5.02(89)	0.02(2)	0.04(6)	0.01(1)	101.16(102)
Gl(10)	63.32(145)	0.09(3)	17.47(42)	1.87(47)	0.05(3)	0.26(7)	1.29(32)	4.59(62)	3.62(22)	0.02(3)	92.58(87)
JN0305e-2k 900°C 1.5 GPa 100 h 0.45Hbl + 0.35Pl + 0.05Grt + 0.15Gl											
Hbl(7)	42.04(176)	1.46(67)	12.99(271)	16.72(294)	0.23(13)	9.2(142)	8.41(98)	3.45(50)	1.02(47)	0.01(1)	95.53(91)
Pl(6)	62.89(255)	0.01(1)	22.36(152)	0.15(11)	0.01(1)	0(0)	3.46(125)	8.88(106)	0.52(11)	0(0)	98.29(124)
Grt(6)	38.79(89)	0.26(10)	21.54(53)	22.94(80)	0.48(23)	2.84(28)	13.84(58)	0.02(2)	0.01(1)	0.01(1)	101.24(130)
Gl(9)	62.39(91)	0.19(12)	17.33(53)	2.85(51)	0.06(3)	0.38(17)	1.83(85)	4.55(23)	3.54(32)	0.01(1)	93.13(83)
JN0305e-3k 950°C 1.5 GPa 101 h 0.23Hbl + 0.21Cpx + 0.1Grt + 0.46Gl											
Hbl(6)	42.00(63)	2.28(41)	13.47(21)	13.45(49)	0.21(2)	12.22(57)	7.36(74)	3.38(15)	0.79(8)	0.09(8)	95.26(62)
Grt(7)	39.04(54)	1.04(7)	19.72(29)	22.74(57)	1.05(5)	8.40(35)	6.54(25)	0.06(2)	0.01(1)	0.02(1)	98.62(55)
Cpx(7)	51.13(93)	0.53(14)	7.07(104)	10.93(144)	0.35(6)	11.50(63)	14.96(117)	1.72(20)	0.03(1)	0.03(4)	98.24(83)
Gl(17)	52.05(157)	0.78(11)	17.82(84)	8.82(72)	0.18(3)	1.87(18)	3.50(16)	4.38(22)	2.68(25)	0.10(31)	92.15(194)

[a] Measurement method: Bulk rock XRF at the Institute of Geology and Geophysics, Chinese Academy of Sciences; minerals and melts: EPMA-1600 at the State Key Laboratory of Ore Deposit Geochemistry, Institute of Geochemistry, Chinese Academy of Sciences. Pl, plagioclase; Hbl, hornblende; Chl, chlorite; Grt, garnet; Cpx, clinopyroxene; Opx, orthopyroxene; Gl, melt. LOI: loss on ignition. Numbers in the brackets behind minerals are points analyzed. All data are in wt.%. Errors in parentheses for compositions are one standard deviation from the mean, reported as least units cited. 47.08 (135) represents (47.08 ± 1.35) wt.%. Total Fe is expressed as FeO*. Italicized notation such as "*JN0305e-1k 850 °C 1.5 GPa 97 h 0.5Hbl + 0.4Pl + 0.02Grt + 0.08Gl*" represents run number, temperature, pressure, run duration, and run products, respectively. The number before each phase is the mode of each phase by point counting, with a statistical error of ±5%.

Table 2
Trace element compositions of the starting material (JN0305e) and run melts (ppm) at 850–950 °C.[a]

	JN0305e	JN0305e-1k	JN0305e-2k	JN0305e-3k
Element	Bulk rock	850 °C (4)	900 °C (5)	950 °C (10)
Rb	31.43	101(2)	78.2(46)	65.6(62)
Sr	823.6	996(32)	849(78)	1067(114)
Y	19.1	4.50(66)	7.34(148)	10.40(240)
Zr	43.85	29.6(44)	72.7(456)	45.6(57)
Nb	9.57	2.59(85)	13.6(53)	10.5(22)
Ba	318.1	1299(29)	907(117)	513(114)
La	31.25	19.3(42)	39.6(108)	34.9(62)
Ce	77.02	38.7(101)	73.5(112)	77.3(163)
Pr	10.3	4.24(131)	7.22(108)	9.70(190)
Nd	43.03	16.5(49)	26.2(40)	37.2(94)
Sm	8.44	2.60(76)	3.46(71)	5.93(164)
Eu	2.35	0.63(16)	0.95(22)	1.89(50)
Gd	6.78	1.67(29)	2.50(45)	3.82(98)
Tb	0.87	0.20(7)	0.28(7)	0.46(12)
Dy	4.26	0.97(17)	1.63(48)	2.29(54)
Ho	0.76	0.17(2)	0.24(7)	0.39(12)
Er	1.89	0.36(9)	0.72(24)	0.92(20)
Tm	0.26	0.06(2)	0.09(3)	0.13(3)
Yb	1.49	0.40(16)	0.70(24)	0.88(22)
Lu	0.22	0.04(1)	0.08(3)	0.10(2)
Hf	1.42	0.96(22)	1.53(74)	1.16(26)
Ta	0.43	0.13(8)	0.46(21)	0.33(8)
Pb	7.78	38.9(15)	57.2(73)	22.7(120)
Th	0.4	0.09(5)	0.33(0.15)	0.25(6)
U	0.14	0.09(3)	0.24(9)	0.13(3)
Sr/Y	43.12	221(42)	116(24)	102(16)
ΣREE	188.91	86(22)	157(26)	182(35)
Eu/Eu*	0.92	0.87(14)	0.95(17)	1.17(11)
$(La/Yb)_n$	14.1	34(19)	41(14)	27(9)

[a] Measurement method: Bulk rock ICP-MS (Finnigan Element) at Institute of Geology and Geophysics, Chinese Academy of Sciences; minerals: LA-ICP-MS, at the State Key Laboratory of Geological Processes and Mineral Resources, China University of Geosciences, Wuhan.

for dehydration melting of amphibolite at 1.0–2.0 GPa, and 800–1000 °C is Hbl + Pl → Cpx + Grt + Gl (melt) (Sen and Dunn, 1994; Wolf and Wyllie, 1991, 1994; Zhang et al., 2013; Zhou et al., 2005). Although the phase relationships, mineral and melt compositions in our experiments show the same reaction, distinct reactions in different stages can be distinguished for an isobaric pressure of 1.5 GPa at 800–950 °C (Fig. 2).

The first stage of the reaction occurs at 800 °C (Fig. 2a):

$$Chl \rightarrow Hbl + H_2O \quad (1)$$

$$Chl + Hbl + Pl \rightarrow Opx + Cpx + Gl \quad (2)$$

The first stage involves the chlorite-out reaction, an increase in Hbl and the generation of melt. The An in Pl increases slightly. Hence, the melt is enriched in SiO_2 and Na_2O.

The second stage of the reaction occurs at 850–900 °C (Fig. 2b and c):

$$Hbl + Pl \rightarrow Grt + Gl \quad (3)$$

At this stage, Hbl and Pl gradually decrease by almost the same amount, along with an obvious increase in melt and generation of Grt. The An in Pl obviously decreases. Thus, with the exception of CaO, the oxide contents in the melt do not change much. However, compared to those in the melt produced at 800 °C, SiO_2, Al_2O_3, CaO, Na_2O, and K_2O contents of melts from 850 to 900 °C runs clearly increase.

The final stage of the reaction occurs at 950 °C (Fig. 2d):

$$Hbl + Pl \rightarrow Grt + Cpx + Gl \quad (4)$$

At this stage, Cpx appears, Pl disappears and Hbl decreases significantly. At same time, Grt increases obviously along with sharp increases in Cpx and melt. Hence, the SiO_2, Na_2O, and K_2O contents of the melt decrease significantly, while the FeO*, MgO, CaO and TiO_2 contents of the melt increase markedly.

4.3. Comparison between the melts and the Mesozoic potassium-rich adakitic rocks

A comparison between the partial melts and the Mesozoic potassium-rich adakitic rocks of the eastern North China Craton can clearly place firm constraints on the origin of these rocks. In particular, in the Zhangjiakou area, three Mesozoic intrusions whose rocks have adakitic features are present in the vicinity of the experimental sample (Fig. 1). They are the Guzuizi granite, the Honghualiang granite and the Zhuanzhilian diorite. These potassium-rich adakitic rocks have been considered to derive from the ancient lower crust that could be represented by the exposed amphibolite and granulites (Jiang et al., 2007). Therefore, more attention has been paid to comparisons between the partial melts and these three Mesozoic potassium-rich adakitic rocks to investigate the origin of the latter. Data on the other potassium-rich adakitic rocks from the eastern North China Craton are the same as those cited by Jiang et al. (2007, and references therein).

4.3.1. Comparison of major elements

The normative Ab–An–Or ternary diagram (Fig. 4) indicates that except for the melt at 800 °C, all the other experimental melts are within the range of the Mesozoic potassium-rich adakitic rocks from the eastern North China Craton. In particular, the run melts at 850 °C and 900 °C have compositions near those of the Guzuizi and Honghualiang granites, and the 950 °C melt composition is close to that of the Zhuanzhilian diorite (Fig. 4). These results indicate that the experimental melts at 850–950 °C are similar to the Mesozoic potassium-rich adakitic rocks from the eastern North China Craton.

In the Harker diagram (Fig. 5), all the components of the 800 °C melts are outside of the ranges for the Mesozoic potassium-rich adakitic rocks, which indicates that the 800 °C melts cannot represent the magma of these adakitic rocks from the eastern North China Craton. This difference may be due to their low melting degree, and the melts could not form magma in the experiment. Except for the 800 °C melts, all the other melts show characteristics in good accordance with those of the Mesozoic potassium-rich adakitic rocks. The contents of SiO_2, K_2O, CaO, FeO*, and MgO in all the run melts between 850 and 950 °C are within the ranges for the Mesozoic potassium-rich adakitic rocks from the eastern North China Craton. A salient feature is that the Al_2O_3 contents of all the melts are higher than those of the Mesozoic potassium-rich adakitic rocks. This contrast is due to factors such as the degree of melting, pressure, and content of Al_2O_3 in the starting material.

Moreover, the changing trend of the melt compositions is basically identical to the trend of the compositional changes in the three intrusions (Guzuizi granite, Honghualiang granite and Zhuanzhilian diorite). The contents of SiO_2, Na_2O, and K_2O decrease while those of CaO, FeO*, and MgO increase with increasing temperature. The SiO_2 contents of the 850–900 °C melts are similar to those of the Guzuizi and Honghualiang granites, whereas the SiO_2 contents of the 950 °C melts are similar to that of the Zhuanzhilian diorite. It should be highlighted that the plots of Na_2O, K_2O, CaO, FeO*, and MgO contents for the melt at 850 °C are close to those of the Honghualiang granite. The composition of the 950 °C melt is close to that of the Zhuanzhilian diorite in K_2O and Na_2O contents, but the former has lower contents of CaO and MgO and higher contents of FeO*and Al_2O_3. The remarkable similarities suggest that the experimental amphibolite and the temperature and pressure conditions are similar to the source and the formation conditions of the three intrusions. The experimental temperature is closely consistent with the temperatures calculated (960 and 967 °C) from the two-pyroxene thermometers for the Zhuanzhilian diorite by Jiang et al. (2007). Overall, the 850–900 °C melt compositions are similar to those of Guzuizi and Honghualiang granites, whereas the 950 °C melt compositions are close to that of the Zhuanzhilian diorite.

Due to the high contents of Fe and the low contents of Mg, the Mg# of in the melts are low, and even the Mg# in melts at 850–950 °C are also within the Mg# range of the Mesozoic potassium-rich adakitic rocks. The

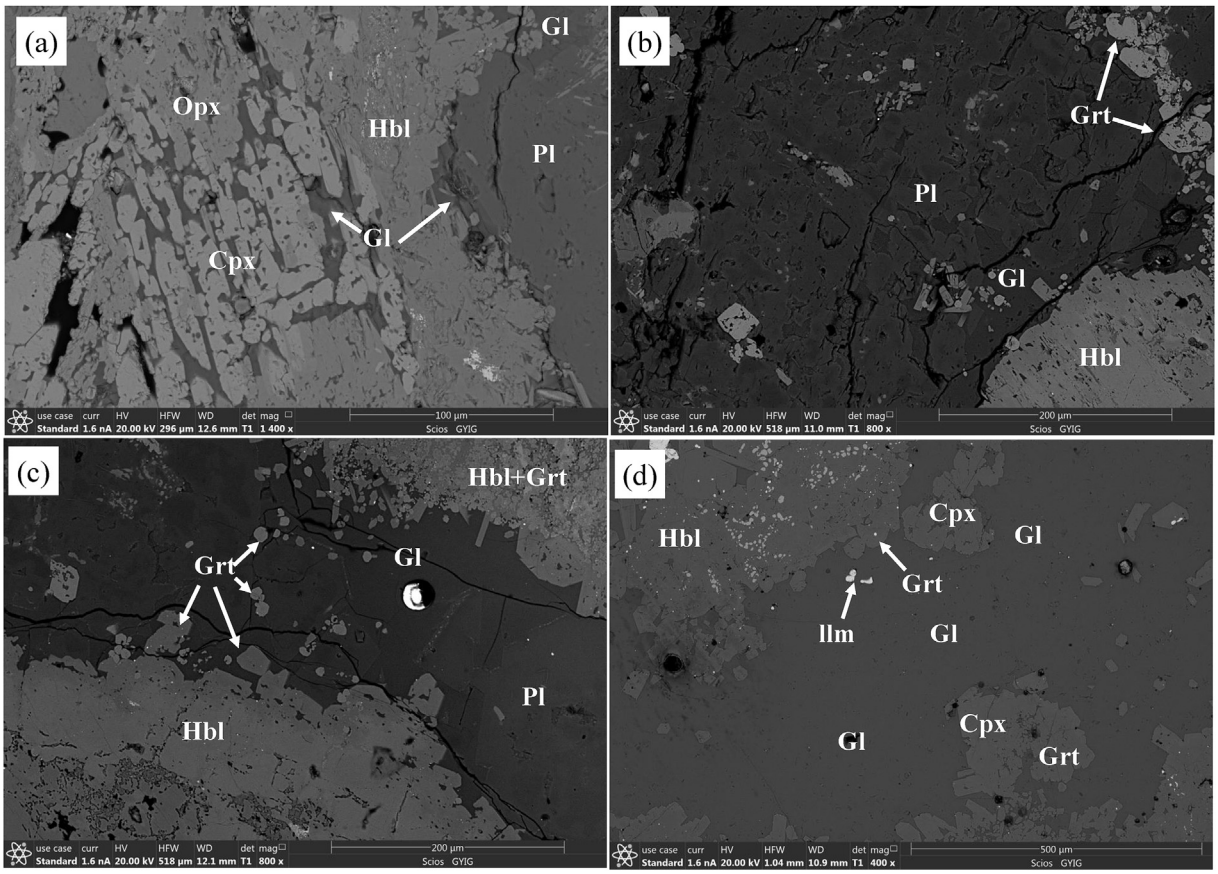

Fig. 2. Backscattered electron images of run products. (a) 800 °C, (b) 850 °C, (c) 900 °C, (d) 950 °C. Pl, plagioclase; Hbl, hornblende; Grt, garnet; Cpx, clinopyroxene; Opx, orthopyroxene; Ilm, Ilmenite; Gl, melt.

Mg# of all melts are significantly lower than those of the three potassium-rich adakitic intrusions in the Zhangjiakou area and fall near the lower boundary of the Mg# range of the Mesozoic potassium-rich adakitic rocks from the eastern North China Craton. Hence, partial melting of amphibolite can produce potassium-rich adakitic rocks with low Mg# only at 1.5 GPa and 850–950 °C. However, if potassium-rich adakites with high Mg# signatures are the products of dehydration melting of amphibolite at 1.5 GPa and 850–950 °C, then the major element data require that the melts interact with wall-rocks with high MgO contents or mix with basaltic magmas during their transport to the surface. The K_2O/Na_2O ratios in the melts at 850–950 °C are also within the range of the Mesozoic potassium-rich adakitic rocks and similar to those of the three potassium-rich adakitic intrusions in the Zhangjiakou area. However, the A/CNK ratios are anomalous to some extent. The A/CNK values of 950 °C melts fall outside the range of the Mesozoic potassium-rich adakitic rocks from the eastern North China Craton. Although the A/CNK values of the melts in 850–900 °C melts are within the range of the Mesozoic potassium-rich adakitic rocks from the eastern North China Craton, they are higher than those of the three Zhangjiakou intrusions and plot at the bottom of the range of the Mesozoic potassium-rich adakitic rocks from the eastern North China Craton. The high Al_2O_3 content in the starting material for the melts is the possible reason for the higher A/CNK ratio in the melts.

4.3.2. Comparison of REEs and trace elements

We chose the 850 °C, 900 °C, and 950 °C melts for trace element analysis by LA-ICP-MS (Table 2). The 800 °C melt is inappropriate for such analysis because of its low contents of trace elements and small volume of melts. Using the trace element characteristics of the Mesozoic intermediate-felsic potassium-rich adakitic rocks from the eastern North China Craton as the background values, we primarily compare the trace element characteristics of the melts and the three intrusions.

The trace elements of potassium-rich adakitic rock are characterized by high Sr content and low Y content. In the graphs of Sr/Y–Y and $(La/Yb)_n$–Yb_n (Fig. 6), the melts at 850–950 °C plot are plotted within the range of the potassium-rich adakite, which is in accord with the results from of Rapp et al. (2002, 2003). Furthermore, the melt plots are distributed among the three Zhangjiakou intrusions (Guzuizi granite, Honghualiang granite, and Zhuanzhilian diorite). Fig. 6 shows that the melt compositions are remarkably similar to those of the Mesozoic potassium-rich adakitic rocks from the eastern North China Craton in terms of $(La/Yb)_n$ and Sr/Y ratios.

The steep REE patterns of the Mesozoic potassium-rich adakitic rocks from the eastern North China Craton (Fig. 7) indicate enrichment in LREEs relative to HREEs and small positive Eu anomalies. The REE patterns of the 850–950 °C melts are in the range of those for the Mesozoic potassium-rich adakitic rocks from the eastern North China Craton and show an overall similarity to the Zhuanzhilian diorite, the Honghualiang granite, and the Guzuizi granite, although their total REEs are slightly different. Compared with those of the three intrusions, the REEs distribution curve of the 950 °C melt, with a small positive Eu anomaly, is similar to that of the Zhuanzhilian diorite, but the total REE content of the melt is lower. In contrast, the Zhuanzhilian diorite shows a slightly negative Eu anomaly. The REE distribution curves of the 900 °C melt and the Guzuizi granite are almost identical. However, the REE contents of the melt are generally higher. The LREE contents of the 900 °C melt are similar to those of the Honghualiang granite, but the HREE contents are considerably higher than those of the latter. The REE distribution curve of the 850 °C melt is similar to that of the Honghualiang granite, although the LREE contents are lower while the HREE contents are higher than those of the latter. In general, Grt is relatively rich in HREEs. Therefore, the HREE contents in the 850 °C and 900 °C melts depend on the contents

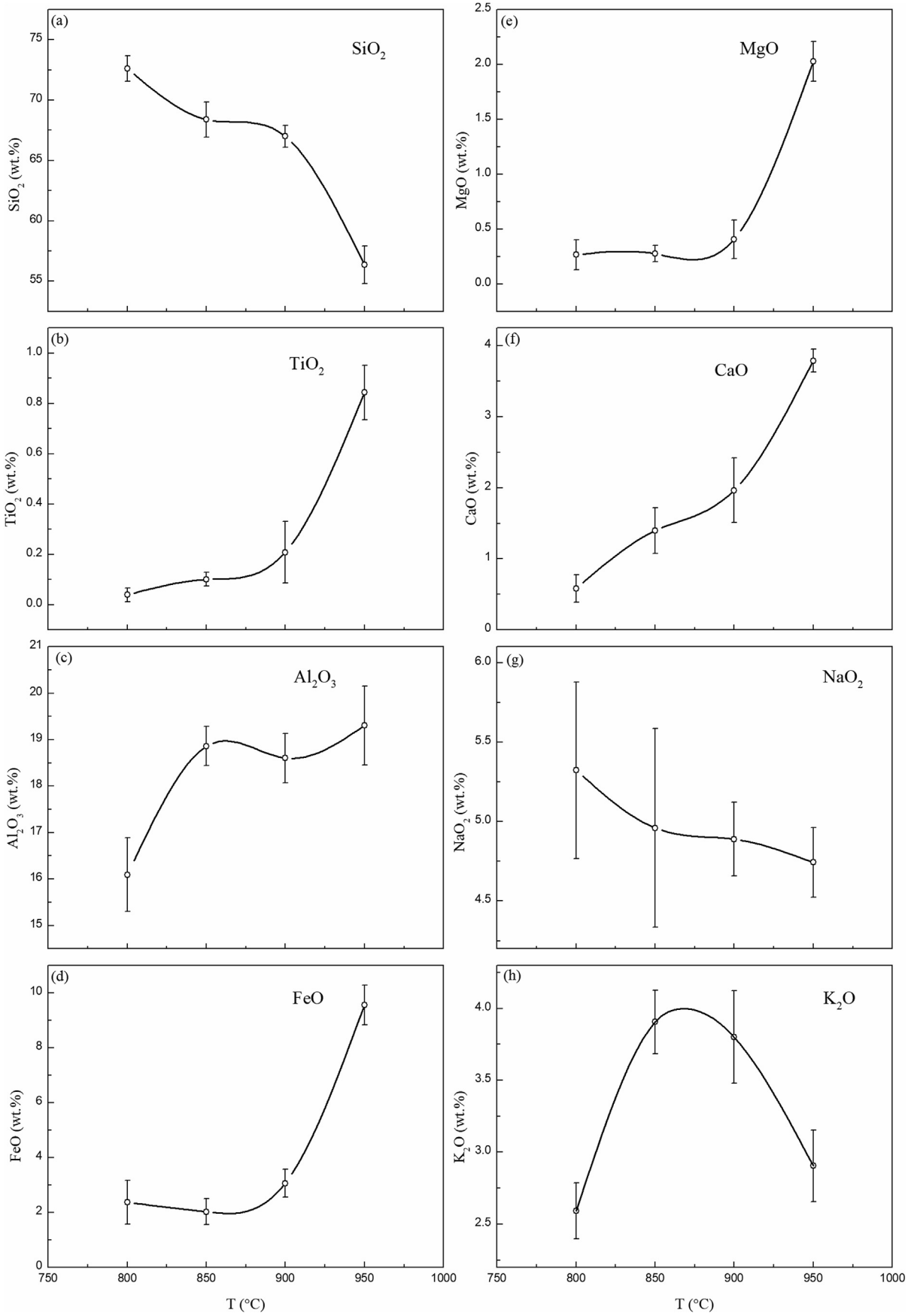

Fig. 3. Variation in melt composition as a function of temperature.

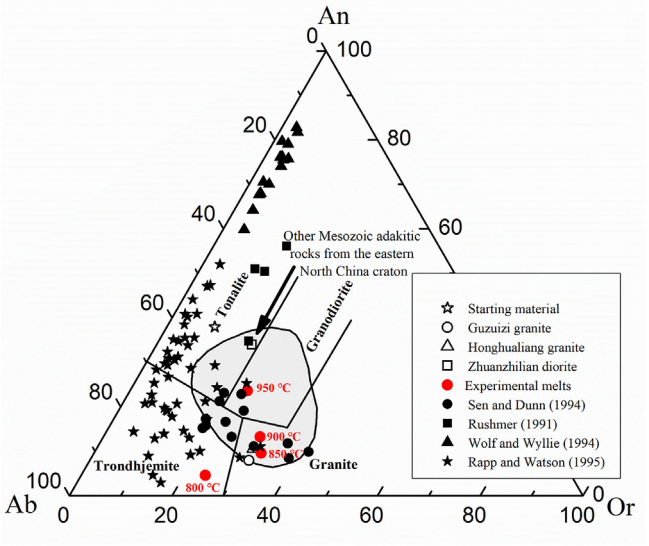

Fig. 4. Normative albite (Ab) – anorthite (An) – orthoclase (Or) diagram for run melts in this study, melts of previous experiments, and Mesozoic potassium-rich adakitic rocks from the eastern North China Craton. The data for the Guzuizi granite, the Honghualiang granite and the Zhuanzhilian diorite are from Jiang et al. (2007). The shaded area represents the range of other Mesozoic adakitic rocks from the eastern North China Craton, and the data are the same as those of Jiang et al. (2007, and references therein).

of newly formed Grt in the run products. The HREE enrichment in these melts compared to the Honghualiang granite may indicate more residual Grt in the source area of the Honghualiang granite.

From the comparison above, the distributions of REEs in the experimental melts are in accord with those of Mesozoic potassium-rich adakitic rocks from the eastern North China Craton.

In the spider diagram of trace elements (Fig. 8), the overall characteristics of the melts are consistent with those of the Mesozoic potassium-rich adakitic rocks from the eastern North China Craton. However, the run melts show slightly lower Ta, Zr, and Hf and significantly lower contents of Th and U than the Mesozoic potassium-rich adakitic rocks from the eastern North China Craton. The contents of Th and U in the starting material are low (Table 2 and Fig. 8), and the contents of Th and U in the residual minerals are also low, mostly below the detection limits, so the severe deficiency may be caused by the low content of Th and U in the starting material. On the other hand, ilmenite (Ilm), as a minor mineral, is observed in the run products (Fig. 2d), and Ta, Zr, and Hf are usually enriched in Ilm (He et al., 2016). Therefore, the slight depletions in Ta, Zr, and Hf may be attributed to the selective enrichment of these elements in Ilm.

In summary, the characteristics of major and trace elements of the experimental melts are very similar to those of the Mesozoic potassium-rich adakitic rocks with low Mg# from the eastern North China Craton and similar to the features of three intrusions from the Zhangjiakou region where the starting material was collected. Hence, it can be deduced that the partial melting of the experimental amphibolite can produce some of the Mesozoic potassium-rich adakitic rocks with relatively low

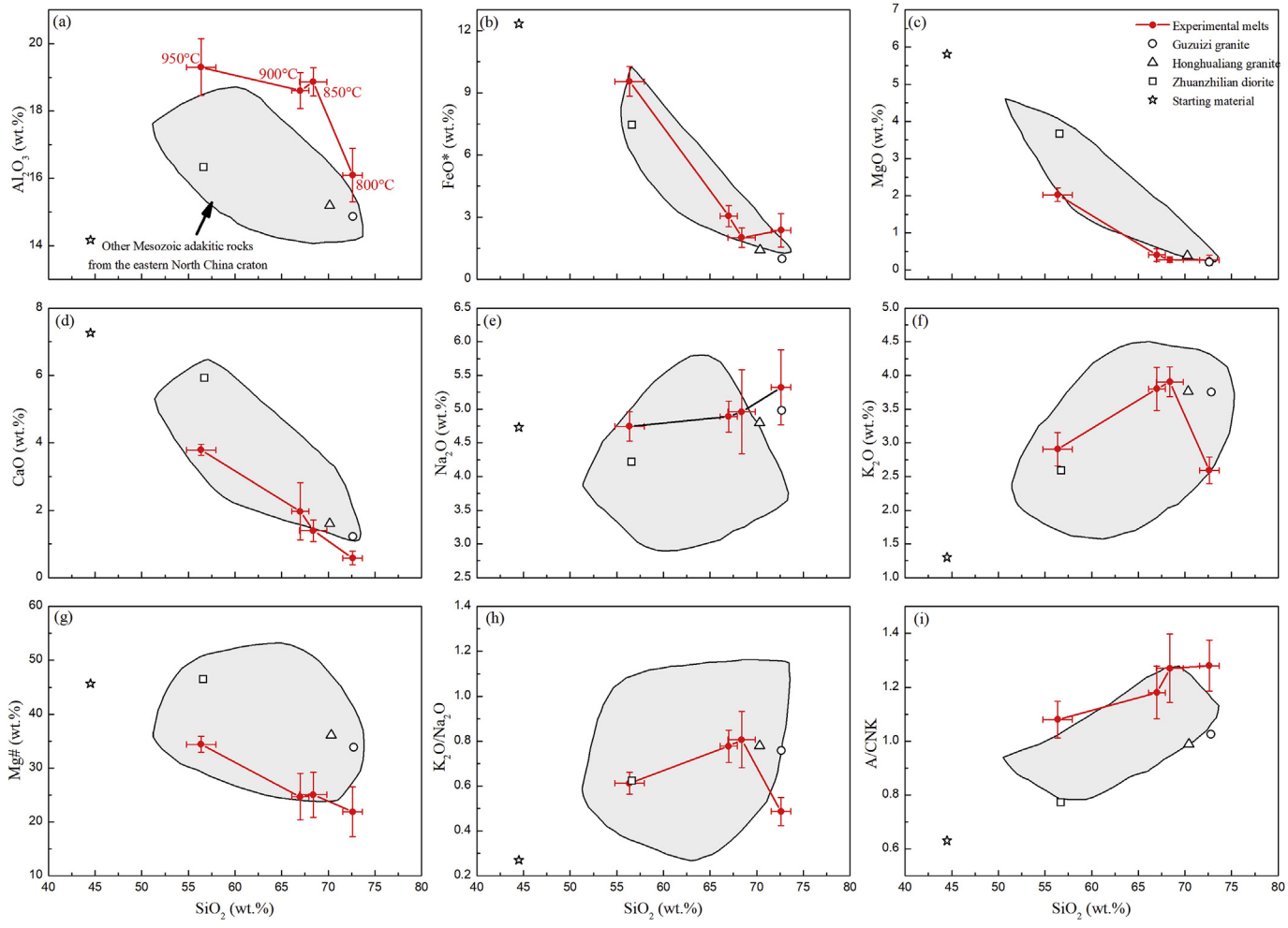

Fig. 5. Comparison of major elements in run melts with those in Mesozoic potassium-rich adakitic rocks from the eastern North China Craton.

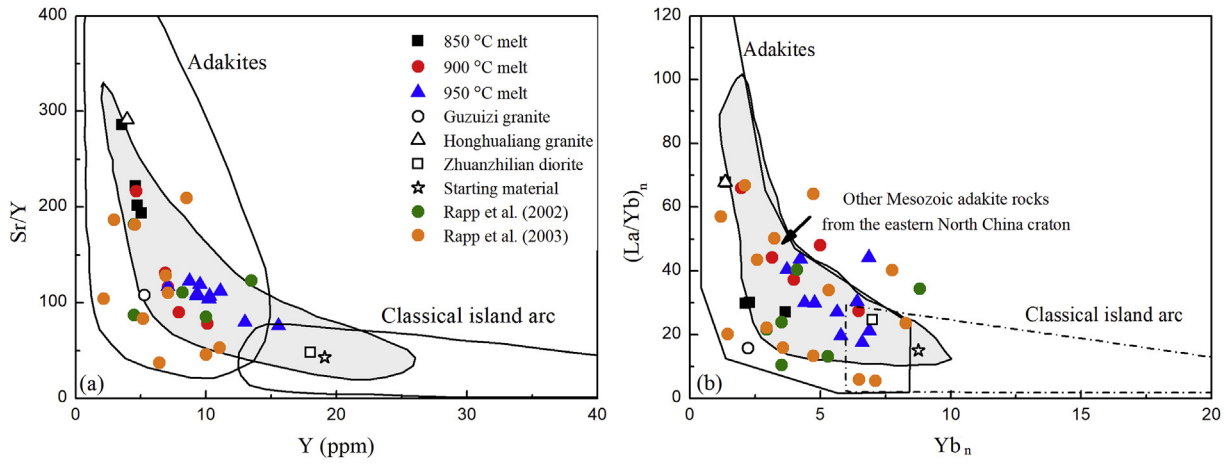

Fig. 6. Sr/Y–Y (a) and $(La/Yb)_n$–Yb_n (b) diagrams for run melts at 850–950 °C, adakites, melts from Rapp et al. (2002, 2003), classic island arcs and Mesozoic potassium-rich adakitic rocks from the eastern North China Craton. The fields of adakites and classic island arcs are cited from Martin (1999).

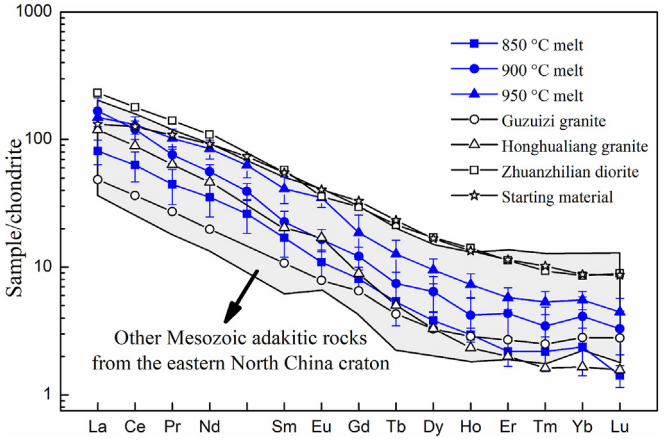

Fig. 7. Comparison of the REE patterns of run melts at 850–950 °C with those of Mesozoic potassium-rich adakitic rocks from the eastern North China Craton. Chondrite values from Sun and McDonough (1989).

Mg# in the eastern North China Craton under the conditions of this experiment. According to the differences between the experimental melts and the Mesozoic potassium-rich adakitic rocks from the eastern North China Craton, if potassium-rich adakitic rocks with high Mg# are directly generated from lower crustal rocks at 1.5 GPa and 850–950 °C, then the actual source rocks may contain higher MgO and lower Al_2O_3 and be more enriched in Th and U than the starting material. However, some previous research proposed another explanation; that is, the potassium-rich adakitic rocks with high Mg# may be derived from lower crustal melts modified by interaction with the wall-rock to acquire their higher MgO contents (Xu et al., 2002, 2008; Gao et al., 2004; Liu et al., 2005).

4.4. Comparison of the experimental restites with the Hannuoba mafic granulite xenoliths

Various lower crustal granulite xenoliths have been found entrained in the Tertiary Hannuoba alkaline basalts adjoining the Mesozoic potassium-rich adakitic rocks in the Zhangjiakou area (Fig. 1). Precambrian zircons are common in mafic granulite xenoliths that have been interpreted to represent portions of the ancient lower crust (Wilde et al., 2003). In addition, some of the Hannuoba mafic granulite xenoliths have Sr–Nd isotope compositions comparable with those of the Mesozoic

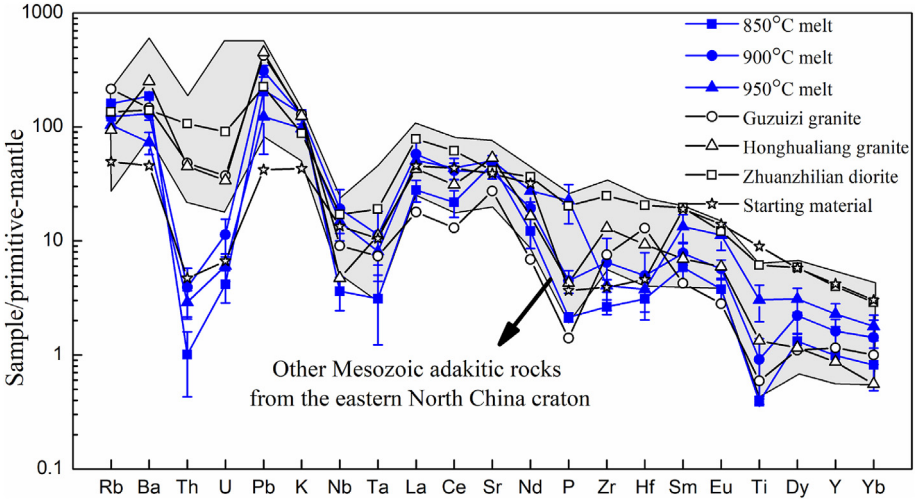

Fig. 8. Comparison of the trace elements of run melts at 850–950 °C with those of Mesozoic potassium-rich adakitic rocks from the eastern North China Craton. Primitive mantle values from Sun and McDonough (1989).

potassium-rich adakitic rocks and the Archean granulite terrains (Liu et al., 2004). Based on these data, Jiang et al. (2007) proposed that the adakitic rocks are formed by partial melting of the ancient lower crust, and that the restites are represented by some of the Hannuoba mafic granulite xenoliths. Next, we compare the experimental restites with the presumed restitic mafic granulite xenoliths.

The Hannuoba mafic granulite xenoliths are dominated by pyroxenes with an assemblage of mainly Cpx + Opx + Pl ± Grt (Zhang et al., 1998; Chen et al., 2001; Liu et al., 2001), contrasting with the assemblages of the experimental restites, which consist of Hbl + Pl + Grt ± Cpx. Chemically, the mafic granulite xenoliths have higher MgO and CaO but lower Al_2O_3 than the experimental restites. Therefore, the Hannuoba mafic granulite xenoliths cannot be the direct products of partial melting of the experimental amphibolite. Liu et al. (2005) argued that intermediate-mafic granulite xenoliths with high Mg# signatures and Ni contents would be formed by melt-rock reactions between a silicic melt and ultramafic country rock (lherzolite). Nevertheless, several other reasons may also explain the differences between the experimental restites and the mafic granulite xenoliths.

First, the experimental partial melts are richer in Al_2O_3 than the Mesozoic adakitic rocks from the eastern North China Craton. Their MgO and CaO contents are at the low end of the range. This result suggests that the Mesozoic potassium-rich adakitic rocks may have been derived from protoliths richer in MgO and CaO and poorer Al_2O_3 than the experimental amphibolite. Compared to Hbl and Chl, Cpx is richer in MgO and CaO and poorer in Al_2O_3. This difference means that the protoliths for the Mesozoic potassium-rich adakitic rocks may have contained Cpx and thus lower Hbl and Chl than the experimental amphibolite. The restites of such protoliths would contain less Hbl, closer to the assemblage of the Hannuoba mafic granulite xenoliths.

Second, the estimated temperatures for the Hannuoba mafic granulite xenoliths (Chen et al., 2001; Liu et al., 2001) are similar to the experimental temperatures. However, the estimated pressures for the Hannuoba mafic granulite xenoliths (typically < 1.2 GPa, Chen et al., 2001) are lower than the experimental pressure. Since Opx tends to increase and Grt tends to decrease with decreasing pressure, this situation may partially explain why the mafic granulite xenoliths contain higher MgO but lower Al_2O_3 than the experimental restites.

Finally, the Zhangjiakou region has undergone multiple episodes of magmatism in the Phanerozoic, as revealed by the Devonian Shuiquangou syenitic complex (Jiang, 2005), the Triassic granites and the Cretaceous diorite (Jiang et al., 2007). The Hannuoba mafic granulite xenoliths are the final products of multiple episodes of magmatism. It is likely that the restitic Hbl from an early partial melting event may have been consumed during later partial melting events. This process may explain the absence of Hbl in the Hannuoba mafic granulite xenoliths.

5. Conclusions

Our experiments demonstrate that partial melting of massive amphibolite at 800–950 °C and 1.5 GPa can produce melts with compositions from granitic to granodioritic. The major and trace element concentrations of the 850–950 °C melts are broadly similar to those of the three Mesozoic adakitic intrusions in the Zhangjiakou area and fall within the ranges of the Mesozoic adakitic rocks in the eastern North China Craton. Thus, the results of this study indicate that partial melting of amphibolite can produce potassium-rich adakitic rocks with low Mg# signatures in the eastern North China Craton under the experimental conditions of 1.5 GPa and 850–950 °C. However, potassium-rich adakitic rocks with high Mg# signatures may not be directly derived from the partial melting of amphibolite. On the other hand, the experimental restites are significantly different from the Hannuoba mafic granulite xenoliths in both mineralogy and geochemistry. The Hannuoba mafic granulite xenoliths cannot represent the direct products of partial melting of the experimental amphibolite.

Declaration of competing interest

The authors declare that they have no known competing financial interests or personal relationships that could have appeared to influence the work reported in this paper.

Acknowledgments

We would like to thank two anonymous reviewers for their thorough and helpful comments. This project was supported by the National Natural Science Foundation of China (Grant Nos. 41772043 and 41802043), the Chinese Academy of Sciences “Light of West China” Program (Dawei Fan, 2017 and Jingui Xu, 2019), and the Youth Innovation Promotion Association CAS (Dawei Fan, 2018434), and the Innovation and Entrepreneurship Funding of High-Level Overseas Talents of Guizhou Province (Dawei Fan, [2019] 10).

References

Atherton, M.P., Petford, N., 1993. Generation of sodium-rich magmas from newly underplated basaltic crust. Nature 362, 144–146.
Beard, J.S., Lofgren, G.E., 1991. Dehydration melting and water saturated melting of basaltic and andesitic greenstones and amphibolites at 1, 3 and 6.9 kb. J. Petrol. 32, 365–401.
Chen, B., Jahn, B.M., Suzuki, K., 2013. Petrological and Nd-Sr-Os isotopic constraints on the origin of high-Mg adakitic rocks from the North China Craton: tectonic implications. Geology 41 (1), 91–94.
Chen, S.H., O'Reilly, S.Y., Zhou, X.H., Griffin, W.L., Zhang, G.H., Sun, M., Feng, J.L., Zhang, M., 2001. Thermal and petrological structure of the lithosphere beneath Hannuoba, Sino-Korean Craton, China: evidence from xenoliths. Lithos 56 (4), 267–301.
Defant, M.J., Drummond, M.S., 1990. Derivation of some modern arc magmas by melting of young subduction lithosphere. Nature 347, 662–665.
Ding, D.S., Chen, L., Gong, E.P., Zhao, X.F., 2019. Zircon U-Pb age, geochemical, and Sr-Nd-O isotopic constraints on the origin of the youngest Mesozoic adakitic dikes in Jiaodong peninsula, North China Craton: implications for Early Cretaceous crustal evolution. Int. Geol. Rev. 175–176, 244–254.
Gao, S., Liu, X., Yuan, H., Hattendorf, B., Günther, D., Chen, L., Hu, S., 2002. Determination of forty-two major and trace elements in USGS and NIST SRM glasses by laser ablation-inductively coupled plasma-mass spectrometry. Geostand. Newsl. 26, 181–196.
Gao, S., Rudnick, R.L., Yuan, H.L., Liu, X.M., Liu, Y.S., Xu, W.L., Ling, W.L., Ayers, J., Wang, X.C., Wang, Q.H., 2004. Recycling lower continental crust in the North China craton. Nature 432, 892–897.
Hawthorne, F.C., Oberti, R., Martin, R.F., Harlow, G.E., Maresch, W.V., Schumacher, J.C., Welch, M.D., 2012. Nomenclature of the amphibole supergroup. Am. Mineral. 97, 2031–2048.
He, X.F., Santosh, M., Ganguly, S., 2017. Mesozoic felsic volcanic rocks from the North China craton: intraplate magmatism associated with craton destruction. Geol. Soc. Am. Bull. 129 (7–8), 947–969.
He, H.L., Yu, S.Y., Song, X.Y., Du, Z.S., Dai, Z.H., Zhou, T., Xie, W., 2016. Origin of nelsonite and Fe–Ti oxides ore of the Damiao anorthosite complex, NE China: evidence from trace element geochemistry of apatite, plagioclase, magnetite and ilmenite. Ore Geol. Rev. 79, 367–381.
Huang, F.A., He, Y.S., 2010. Partial melting of the dry mafic continental crust: implications for petrogenesis of C-type adakites. Chin. Sci. Bull. 55 (22), 2428–2439.
Jiang, N., 2005. Petrology and geochemistry of the Shuiquangou syenitic complex, northern margin of the North China craton. J. Geol. Soc. 162, 203–215.
Jiang, N., Liu, Y.S., Zhou, W.G., Yang, J.H., Zhang, S.Q., 2007. Derivation of Mesozoic adakitic magmas from ancient lower crust in the North China craton. Geochem. Cosmochim. Acta 71, 2591–2608.
Kay, R.W., 1978. Aleutian magnesian andesites–melts from subducted Pacific ocean crust. J. Volcanol. Geoth. Res. 4, 117–132.
Liu, J., Zhang, J., Liu, Z.H., Yin, C.Q., Zhao, C., Peng, Y.B., 2018. Petrogenesis of Jurassic granitoids at the northeastern margin of the North China Craton: new geochemical and geochronological constraints on subduction of the Paleo-Pacific Plate. J. Asian Earth Sci. 158, 287–300.
Liu, Y.S., Gao, S., Jin, S., Hu, S.Y., Sun, M., Zhao, Z.B., Feng, J.L., 2001. Geochemistry of lower crustal xenoliths from Neocene Hannuoba basalt, North China craton: implications for petrogenesis and lower crustal composition. Geochem. Cosmochim. Acta 65, 2589–2604.
Liu, Y.S., Gao, S., Yuan, H.L., Zhou, L., Liu, X.M., Wang, X.C., Hu, Z.C., Wang, L.S., 2004. U–Pb zircon ages and Nd, Sr, and Pb isotopes of lower crustal xenoliths from North China Craton: insights on evolution of lower continental crust. Chem. Geol. 211, 87–109.
Liu, Y.S., Gao, S., Aeolus Lee, C.-T.A., Hua, S.H., Liu, X.M., Yuan, H.L., 2005. Melt–peridotite interactions: links between garnet pyroxenite and high-Mg# signature of continental crust. Earth Planet Sci. Lett. 234, 39–57.

Ma, Q., Zheng, J.P., Xu, Y.G., Griffin, W.L., Zhang, R.S., 2015. Are continental "adakites" derived from thickened or foundered lower crust? Earth Planet Sci. Lett. 419, 125–133.

Macpherson, C.G., Dreher, S., Matthew, T., Thirlwall, F., 2006. Adakites without slab melting: high pressure differentiation of island arc magma, Mindanao, the Philippines. Earth Planet Sci. Lett. 243, 581–593.

Martin, H., 1999. Adakitic magmas: modern analogues of Archean granitoids. Lithos 46, 411–429.

Morgan, G.B. VI, London, D., 2005. Effect of current density on the electronmicroprobe analysis of alkali aluminosilicate glasses. American Mineralogist 90, 1131–1138.

Qian, Q., Hermann, J., 2013. Partial melting of lower crust at 10-15 kbar: constraints on adakite and TTG formation. Contrib. Mineral. Petrol. 165, 1195–1224.

Rapp, R.P., Watson, E.B., Miller, C.F., 1991. Partial melting of amphibolite/eclogite and the origin of Archean trondhjemites and tonalites. Precambrian Res. 51, 1–25.

Rapp, R.P., Watson, E.B., 1995. Dehydration melting of metabasalt at 8–32 kbar: implications for continental growth and crust-mantle recycling. J. Petrol. 36 (4), 891–931.

Rapp, R.P., Xiao, L., Shimizu, N., 2002. Experimental constraints on the origin of potassium-rich adakites in eastern China. Acta Ecol. Sin. 18, 293–302.

Rapp, R.P., Shimizu, N., Norman, M.D., 2003. Growth of early continental crust by partial melting of eclogite. Nature 425, 605–609.

Rushmer, T., 1991. Partial melting of two amphibolites: contrasting experimental results under fluid-absent condition. Contrib. Mineral. Petrol. 107, 41–59.

Sato, M., Shuto, K., Uematsu, M., Takahashi, T., Ayabe, M., Takanashi, K., Ishimoto, H., Kawabata, H., 2013. Origin of late oligocene to middle miocene adakitic andesites, high magnesian andesites and basalts from the back-arc margin of the SW and NE Japan arcs. J. Petrol. 54 (3), 481–524.

Sen, C., Dunn, T., 1994. Dehydration melting of a basaltic composition amphibolite at 1. 5 and 2. 0 GPa: implications for the origin of adakites. Contrib. Mineral. Petrol. 117, 394–409.

Sun, S., McDonough, W.F., 1989. Chemical and isotopic systematics of oceanic basalts: implications for mantle composition and processes. In: Saunders, A.D., Norry, M.J. (Eds.), Magmatism in the Ocean Basins, Spec. Publ. 42. The Geological Society of London, pp. 313–345.

Wang, Q., McDermott, F., Xu, J.F., Bellon, H., Zhu, Y.T., 2005. Cenozoic K-rich adakitic volcanic rocks in the Hohxil area, northern Tibet: lower-crustal melting in an intracontinental setting. Geology 33, 465–468.

Winther, K.T., 1996. An experimental based model for the origin of tonalitic and trondhjemitic melts. Chem. Geol. 127, 43–59.

Wolf, M.B., Wyllie, P.J., 1991. Dehydration melting of solid amphibolite at 10 kbar: textural development, liquid interconnectivity and applications to the segregation of magmas. Mineral. Petrol. 44, 151–179.

Wolf, M.B., Wyllie, P.J., 1994. Dehydration-melting of amphibolite at 10 kbar: the effects of temperature and time. Contrib. Mineral. Petrol. 115, 369–383.

Wilde, S.A., Zhou, X.H., Nemchin, A.A., Sun, M., 2003. Mesozoic crust-mantle interaction beneath the North China craton: a consequence of the dispersal of Gondwanaland and accretion of Asia. Geology 31, 817–820.

Xie, H.S., Zhang, Y.M., Xu, H.G., 1993. A new method of measurement for elastic wave velocities in minerals and rock at high T and P and its significance. Sci. China, Ser. A 36 (10), 1276–1280.

Xiong, X.L., Liu, X.C., Zhu, Z.M., Li, Y., Xiao, W.S., Song, M.S., Zhang, S., Wu, J.H., 2011. Adakitic rocks and destruction of the North China Craton: evidence from experimental petrology and geochemistry. Sci. China Earth Sci. 54 (6), 858–870.

Xu, J.F., Shinjo, R., Defant, M.J., Wang, Q.A., Rapp, R.P., 2002. Origin of Mesozoic adakitic intrusive rocks in the Ningzhen area of east China: partial melting of delaminated lower continental crust? Geology 30, 1111–1114.

Xu, W.L., Hergt, J.A., Gao, S., Pei, F.P., Wang, W., Yang, D.B., 2008. Interaction of adakitic melt-peridotite: implications for the high-Mg# signature of Mesozoic adakitic rocks in the eastern North China Craton. Earth Planet Sci. Lett. 265 (1–2), 123–137.

Yang, D.B., Xu, W.L., Zhao, G.C., Huo, T.F., Shi, J.P., Yang, H.T., 2016. Tectonic implications of Early Cretaceous low-Mg adakitic rocks generated by partial melting of thickened lower continental crust at the southern margin of the central North China Craton. Gondwana Res. 38, 220–237.

Zhang, C., Holtz, F., Koepkea, J., Eric Wolff, P.E., Changqian Ma, C.Q., Jean, H., Bédard, J.H., 2013. Constraints from experimental melting of amphibolite on the depth of formation of garnet-rich restites, and implications for models of Early Archean crustal growth. Precambrian Res. 231, 206–217.

Zhang, G.H., Zhou, X.H., Sun, M., Chen, S.H., Feng, J.L., 1998. Highly chemical heterogeneity in the lower crust and crust-mantle transitional zone: geochemical evidences from xenoliths in Hannuoba basalt, Hebei province. Geochimica 27, 153–169 (in Chinese).

Zhou, W.G., Xie, H.S., Liu, Y.G., Zheng, X.G., Zhao, Z.D., Zhou, H., 2005. Dehydration melting of solid amphibolite at 2.0 GPa: effects of time and temperature. Science in China (Series D) 48 (8), 1120–1133.